This article was downloaded by:
On: *14 January 2011*
Access details: *Access Details: Free Access*
Publisher *Taylor & Francis*
Informa Ltd Registered in England and Wales Registered Number: 1072954 Registered office: Mortimer House, 37-41 Mortimer Street, London W1T 3JH, UK

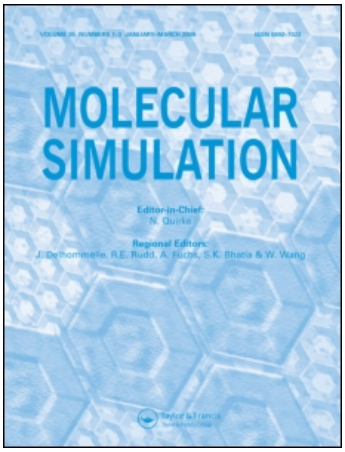

Molecular Simulation
Publication details, including instructions for authors and subscription information:
http://www.informaworld.com/smpp/title~content=t713644482

Application of Gibbs Ensemble and NPT Monte Carlo Simulation to the Development of Improved Processes for H_2S-rich Gases

Philippe Ungerer[ab]; Aurélie Wender[a]; Grégoire Demoulin[a]; Émeric Bourasseau[b]; Pascal Mougin[a]
[a] Institut Français du Pétrole, Rueil-Malmaison Cedex, France [b] laboratoire de Chimie Physique, Université de Paris Sud, Orsay Cedex, France

To cite this Article Ungerer, Philippe , Wender, Aurélie , Demoulin, Grégoire , Bourasseau, Émeric and Mougin, Pascal(2004) 'Application of Gibbs Ensemble and NPT Monte Carlo Simulation to the Development of Improved Processes for H_2S-rich Gases', Molecular Simulation, 30: 10, 631 — 648
To link to this Article: DOI: 10.1080/08927020410001709299
URL: http://dx.doi.org/10.1080/08927020410001709299

PLEASE SCROLL DOWN FOR ARTICLE

Full terms and conditions of use: http://www.informaworld.com/terms-and-conditions-of-access.pdf

This article may be used for research, teaching and private study purposes. Any substantial or systematic reproduction, re-distribution, re-selling, loan or sub-licensing, systematic supply or distribution in any form to anyone is expressly forbidden.

The publisher does not give any warranty express or implied or make any representation that the contents will be complete or accurate or up to date. The accuracy of any instructions, formulae and drug doses should be independently verified with primary sources. The publisher shall not be liable for any loss, actions, claims, proceedings, demand or costs or damages whatsoever or howsoever caused arising directly or indirectly in connection with or arising out of the use of this material.

Molecular Simulation, VOL. 30 (10), 30 August 2004, pp. 631–648

Taylor & Francis
Taylor & Francis Group

Application of Gibbs Ensemble and NPT Monte Carlo Simulation to the Development of Improved Processes for H_2S-rich Gases

PHILIPPE UNGERER[a,b,*], AURÉLIE WENDER[a], GRÉGOIRE DEMOULIN[a], ÉMERIC BOURASSEAU[b] and PASCAL MOUGIN[a]

[a]*Institut Français du Pétrole, 1–4 avenue de Bois Préau, 92852 Rueil-Malmaison Cedex, France;* [b]*Université de Paris Sud, laboratoire de Chimie Physique, bâtiment 349, 91405 Orsay Cedex, France*

(Received December 2003; In final form March 2004)

Downloaded At: 18:29 14 January 2011

The design of improved processes for producing hydrogen sulphide (H_2S)-rich natural gases faces a general scarcity of experimental data, because of the high toxicity and corrosive character of H_2S. We present here a prospective application of Monte Carlo simulation to predict desired fluid properties.

A first step was the selection of intermolecular potentials for water, H_2S, carbon dioxide (CO_2) and methane on the basis of pure component properties (vapour pressures, vapourisation enthalpies, liquid densities, supercritical densities at high pressure). A second step involved the prediction of phase diagrams of binary and ternary mixtures of the methane–H_2S–water system, using two-phase and three-phase Gibbs ensemble simulations. In a third step the density and excess enthalpy of the CO_2–H_2S system were computed for a large range of pressure, temperature and compositions.

Comparison with available experimental data showed that all investigated properties could be consistently predicted without needing parameter calibration on binary data. The results also provided a qualitative understanding of water solubility in H_2S-rich fluids based on molecular self-association.

Keywords: Hydrogen sulphide; Water; Methane; Carbon dioxide; Computer simulation (MC and MD); Phase equilibrium

INTRODUCTION

Natural gases containing more than 10% of hydrogen sulphide (H_2S) cause specific production difficulties. A first type of difficulty arises from the cost of the amine separation unit which is classically used to reduce H_2S content to the specification level. Then, the separated H_2S must be converted to elementary sulfur through Claus units. Thus several important natural gas deposits cannot be produced with a reasonable profitability.

In order to reduce production costs, the performing of a preliminary separation is considered, so that most of the H_2S content of the gas is recovered in the liquid state, allowing its reinjection in deep reservoirs. This reduces the size of the amine separation unit—which is still necessary to meet specification on H_2S content— and of the associated Claus unit. The lower cost of these units compensates largely for the additional cost of the proposed preliminary separation [1,2]. The preliminary separation is performed by a stripper in which the natural gas stream is contacted with the refrigerated recycled stream containing mostly H_2S and water separated. The preliminary treatment operates at a pressure sufficiently high (typically 7 MPa) that the H_2S-rich effluent is in the liquid phase, allowing efficient pumping for reinjection. As far as possible, it is attempted to recover water and carbon dioxide (CO_2) simultaneously with H_2S to reinject them as well in the reservoir (Fig. 1).

The design of such a process faces a general scarcity of experimental data, because the high toxicity and corrosive character of H_2S makes experimental measurements difficult and costly, especially at high pressure.

A first type of missing data relates to the phase equilibria involving methane, H_2S and water at high pressure. The general behaviour is known for the binary systems methane–water [3,4], H_2S–water [4,5], and methane–H_2S [6,7]. However, we suspect that liquid–liquid phase split could occur at a low

*Corresponding author. Address: Institut Français du Pétrole, 1–4 avenue de Bois Préau, 92852 Rueil-Malmaison Cedex, France. E-mail: philippe.ungerer@ifp.fr

ISSN 0892-7022 print/ISSN 1029-0435 online © 2004 Taylor & Francis Ltd
DOI: 10.1080/08927020410001709299

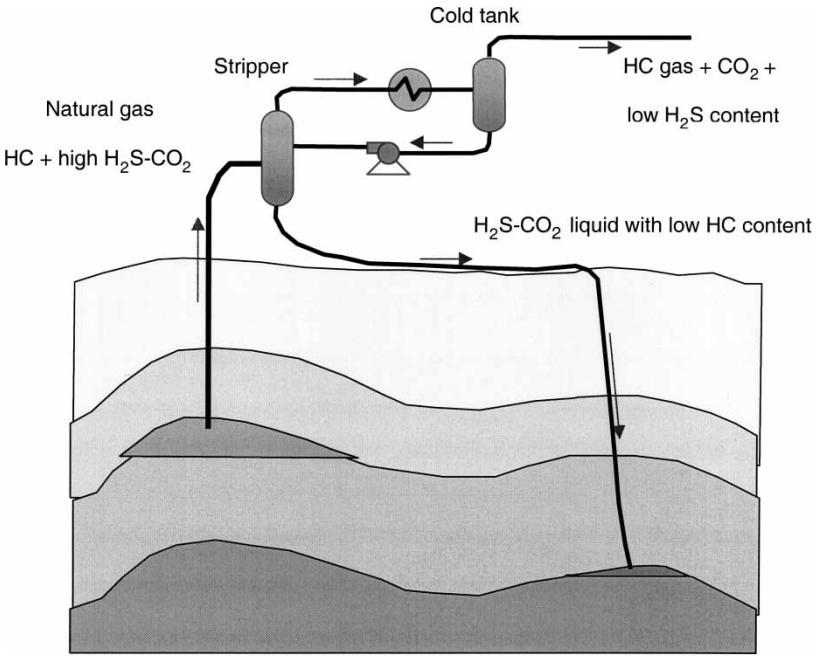

FIGURE 1 General scheme of acid gas preliminary treatment and reinjection.

Downloaded At: 18:29 14 January 2011

temperature in the H_2S–methane system at high pressure, and there are no public data covering such conditions. There are no experimental data about the ternary system methane–water–H_2S. A second type of missing data concerns the enthalpies of mixing, which may influence the energy balance in the separation units. Finally, a last type of missing information relates to the volumetric behaviour of H_2S-rich mixtures at pressures representative of possible reinjection conditions, i.e. up to 80 MPa.

Predicting the desired properties solely from equations of state or from other classical thermodynamic models (such as group-contribution based excess Gibbs energy models) would be risky, because these models are known to be poorly predictive for mixtures involving such polar components as water and H_2S.

Molecular simulation is thus considered as a possible tool to provide more reliable prediction, as illustrated by its capacity to predict reasonably the water solubility of light hydrocarbons [8–10]. Its fundamental advantage is that it accounts for the various types of energy contributing to fluid behaviour. In the particular case of the systems considered here, it makes an explicit account of the electrostatic energy due to the dipole moments of polar molecules (H_2S, water) and of the quadrupole moment of CO_2. As electrostatic forces have a longer range of interaction than the dispersion and repulsion forces which dominate the behaviour of non-polar or slightly polar molecules, this feature is presumed important to quantify interaction energies over a large density range, from the low density of pure methane at moderate pressure to the high density of CO_2 or water in the liquid phase. Another fundamental advantage of molecular simulation is that it accounts for molecular geometry. At first glance, this feature may seem irrelevant in the case of small molecules that are often considered as rigid bodies. However, the way these molecules can arrange in preferred molecular associations may also exert a strong influence on thermodynamic properties. This is particularly the case when water is present, because of the strength of hydrogen bonding. An illustration of the capability of molecular simulation is provided by the water–H_2S system, where the liquid–vapour phase diagram is well predicted without binary parameter fitting [11].

The purpose of the work presented here is the prediction of phase equilibria and various thermodynamic properties in the context of an industrial project. This means that we will mostly rely on existing algorithms and available intermolecular potentials, so that simulation results can be obtained rapidly. As a consequence of the small size of the molecules considered, computer time is expected to be moderate. Also, we will pay particular attention to the validation of simulation results against experimental data. Among the properties investigated, we will mostly concentrate on phase diagrams, density, excess volume, excess enthalpy and derivative properties (such as the isothermal compressivity or the Joule–Thomson coefficient). The reason why we are particularly interested in volumetric properties (density, compressibility, thermal expansion) is that the necessary reinjection pressure depends strongly on liquid density for deep wells. The motivation for investigating excess

enthalpy and Joule–Thomson coefficient at high pressure is the prediction of the thermal regime of reinjection wells.

The article is organised as follows. In a first section, we will expose the Gibbs ensemble Monte Carlo technique [12] that we have used to compute phase equilibria with specific adaptations to consider three-phase equilibria and to improve the efficiency of transfer moves in the Gibbs ensemble. We will also describe the procedure followed to evaluate derivative properties, excess volumes and excess enthalpies. In a second section, we will test intermolecular potentials from the literature on the basis of pure component properties. We will use literature parameters, except for CO_2 whose potential will be slightly reparametrised to provide a better account of the volumetric properties in the supercritical region. The third section is related to the phase behavior of binary and ternary mixtures in the methane–water–H_2S system, without changing potential parameters. The fourth section will be devoted to the prediction of densities and excess properties, mainly in the H_2S–CO_2 system. As combining rules appear to exert a strong influence in this system, we will perform a specific analysis regarding their selection prior to making predictions. Finally, a general discussion will be provided in the fifth section to discuss the capability of molecular simulation to quantitatively predict properties. This will be also the opportunity to propose molecular explanations for some specific features of the systems considered.

Downloaded At: 18:29 14 January 2011

SIMULATION METHODS

NPT and Gibbs Ensemble Simulation Methods

In order to compute phase properties such as densities and enthalpies we used NPT Monte Carlo simulations implemented with a cubic simulation box and periodic boundary conditions [13,14]. The elementary moves involved were molecular translations and rotations, with equal frequencies, and volume changes with a frequency approximately equal to $1/N$, where N is the number of molecules of the simulation box. Internal moves are not necessary because all the molecules considered have been considered rigid.

When computing phase equilibria, we used the Gibbs ensemble technique [12]. Alternative methods like histogram reweighting [15] or Gibbs–Duhem integration might have been more efficient for pure components or binary mixtures, but would have been difficult to implement in the case of ternary systems. The two-phase Gibbs ensemble has been used either at constant volume to compute vapour–liquid equilibrium properties of pure compounds, or at imposed pressure to compute either vapour–liquid or liquid–liquid equilibria of binary systems. The Gibbs ensemble technique has been applied to three-phase equilibria, using the same Monte Carlo moves to perform molecule transfers between simulation boxes or volume changes. As a result of the phase rule, three-phase Gibbs ensemble calculations have been used either at imposed volume when computing vapour–liquid–liquid coexistence properties of binary systems, or at imposed pressure when considering ternary systems. In addition to the translation and rotation moves, the Gibbs ensemble requires concerted volume changes in the case of simulations at imposed global volume, and transfer moves. In order to increase the acceptance rate of transfer moves, which tends to be very low in dense liquids, we have implemented a statistical bias recently proposed for cyclic alkanes [16]. Its purpose, inspired from previous algorithms [17], is to select a suitable site by several insertions of a Lennard–Jones sphere in a first stage, and to test various orientations and conformations at the selected location in the second stage. Although the molecules considered here do not display several conformations, the algorithm is very efficient because the site selection of the first stage is rather rapid, and allows us to reserve the more expensive evaluation of the electrostatic forces to more favorable sites in the second stage.

The interaction energy has been considered as the sum of Lennard–Jones and electrostatic energies, using electrostatic partial charges for dipolar or quadrupolar molecules (water, H_2S, CO_2).

The Lennard–Jones energy was computed using standard long range corrections with a cut-off radius set either to a fixed distance or to the half of the box length. Unless stated otherwise, cross Lennard–Jones parameters were determined with the Lorentz–Berthelot combining rules. In specific cases, we used also the combining rules of Kong [18] and Waldmann–Hagler, as cited by Delhommelle and Millié [19].

The electrostatic energy arising from the partial point charges was computed from two methods. In the first method, we simply applied the Coulomb equation, neglecting the electrostatic interactions between molecules whose centers of mass are separated by more than the cut-off radius. In a second method, we used Ewald summation [13] which is characterised by two numerical parameters: a real range parameter α involved in the real space sums, which is homogeneous to an inverse length, and an integer parameter k_{max} which defines the range of integration in the reciprocal space. As we will discuss it along with the selection of intermolecular potentials, the first method has been used in most cases, and the second method has been used for tests with pure water only.

Derivative Properties

We here term derivative properties those obtained as second order derivatives of the Gibbs energy. They comprise, *inter alia*, the isothermal compressibility coefficient:

$$\beta_T = -\frac{1}{V}\left(\frac{\partial V}{\partial P}\right)_T,$$

the isobaric thermal expansivity $\alpha_P = 1/V(\partial V/\partial T)_P$ and the heat capacity $C_P = (\partial H/\partial T)_P$ where V is volume and H is enthalpy. As briefly discussed by Jorgensen [20] and further developed by Lagache and coworkers [21] it is possible to analyse statistical fluctuations in the NPT ensemble to obtain these properties from Monte Carlo simulations.

Since Monte Carlo methods do not calculate the kinetic energy, we can use them only to calculate residual properties (deviation from ideal gas properties). This is sufficient to compute isobaric thermal expansivity and isothermal compressivity, but not heat capacities. This is why we need ideal gas capacities from experimentally-based correlations [22] to determine these properties. For mixtures, ideal heat capacities may be obtained from mole average of pure component properties. As a result, only pure component properties are used in the process of evaluating derivative properties from Monte Carlo simulation.

The Joule–Thomson coefficient $\mu_{JT} = (\partial T/\partial P)_H$ is obtained as a combination of molar volume, isobaric thermal expansivity and heat capacity.

The computation of derivative properties does not require a significant computational overhead in Monte Carlo simulations, but longer runs are needed to obtain a satisfactory accuracy.

Excess Properties

The molar excess volume V^E in a binary mixture of molar volume V is

$$V^E = V - x_1V_1 - (1 - x_1)V_2 \tag{1}$$

where the subscripts 1 and 2 refer to pure component, x is mole fraction and V is molar volume, all volumes being taken in the same P, T conditions. This expression allows excess volume to be readily computed from Monte Carlo simulation results.

Similarly, the molar excess enthalpy in a binary system is:

$$H^E = H - x_1H_1 - (1 - x_1)H_2 \tag{2}$$

where $H = U_{ext} + U_{int} + K + PV$ is the enthalpy, U_{ext} is the intermolecular potential energy, U_{int} is the molar internal potential energy and K is the kinetic energy of the system, these properties being defined per mole of substance for either pure components or the mixture, at the same temperature and pressure.

The computation of excess enthalpy is somewhat more delicate in principle, because the kinetic part of energy is not considered in Monte Carlo simulation [21,23]. Also, we neglect the internal energy of the molecules because we consider them as rigid in the course of this study. Monte Carlo results allow us only to compute the configurational enthalpy $\hat{H} = U_{ext} + PV$. The molar total enthalpy may be expressed as the sum of the molar configurational enthalpy $\hat{H}$ and the molar ideal gas energy $E^{id} = U_{int} + K$:

$$H = \hat{H} + E^{id} \tag{3}$$

The ideal gas energy of the mixture is obtained from the mole average of the pure component contributions:

$$E^{id} = x_1E_1^{id} + (1 - x_1)E_2^{id} \tag{4}$$

so that the molar excess enthalpy is:

$$H^E = \hat{H} - x_1\hat{H}_1 - (1 - x_1)\hat{H}_2 \tag{5}$$

This expression allows us to evaluate easily the excess enthalpy from Monte Carlo simulations. Note however that we have implicitly assumed that the average internal potential energy per molecule is the same in the pure components and in the mixture. This might be untrue for large flexible molecules which adopt different internal conformations according to their environment.

The calculation of excess volume and excess enthalpy can be implemented in two ways. The first way consists in performing three NPT simulations considering respectively the pure components and the mixture in the same P, T conditions, so that Eqs. (1) and (5) can be readily used. This method may be applied to equilibrium conditions or inside the monophasic region as well. The second way, which is possible only in equilibrium conditions of binary mixtures at imposed temperature and pressure, takes advantage of the initialisation of the Gibbs ensemble technique. It consists in initialising each simulation box with a pure component, and performing first a run without molecule transfer moves between phases. It is thus possible to obtain V_1, V_2, $\hat{H}_1$ and $\hat{H}_2$. Then, transfer moves are implemented so that V and $\hat{H}$ may be computed for the desired phase, once the system has equilibrated. Both methods have been used in this study.

SELECTION OF INTERMOLECULAR POTENTIALS

Methane

In the present study, we are mostly interested in a temperature range where methane is supercritical.

Downloaded At: 18:29 14 January 2011

TABLE I Parameters of the intermolecular potential models investigated in the present study for the various components. The force centres and charges are either located on atomic nuclei (C, S, H, O) or on intermediate points (M).

	Force centre or charge	Position (Å)			Lennard–Jones parameters		Charge (q/e)	References
		X	Y	Z	ε/k (K)	σ (Å)		
CH_4	C	0	0	0	149.92	3.7327	0	[24]
H_2S	S	0	0	0	250	3.73	0.40	[27]
	H1	0.9639	0.9308	0			0.25	
	H2	−0.9639	0.9308	0			0.25	
	M	0	0.1862	0			−0.9	
H_2O (TIP4P)	O	0	0	0	78.03	3.1536	0	[29]
	M	0.15	0	0			−1.04	
	H1	0.5859	0.757	0			0.52	
	H2	0.5859	−0.757	0			0.52	
CO_2 (EPM2)	C	0	0	0	28.129	2.757	0.6512	[37]
	O1	1.149	0	0	80.507	3.033	−0.3256	
	O2	−1.149	0	0	80.507	3.033	−0.3256	
CO_2 (Vrabec)	M1	1.2088	0	0	133.22	2.9847	–	[38]
	M2	−1.2088	0	0	133.22	2.9847	–	
	C	0	0	0	–	–	3.1597	
	M3	−0.5	0	0	–	–	−1.57985	
	M4	0.5	0	0	–	–	−1.57985	
CO_2 (EPM-W)	C	0	0	0	28.999	2.785	0.6645	This study
	O1	1.16	0	0	81.23	3.0356	−0.33225	
	O2	−1.16	0	0	81.23	3.0356	−0.33225	

Downloaded At: 18:29 14 January 2011

Therefore, the intermolecular potential must not only account for the liquid–vapour equilibrium properties of pure methane, but also for its supercritical behaviour. The Lennard–Jones 6–12 potential of Möller [24], whose parameters are recalled in Table I, has been shown to describe very well pure methane density at pressures up to 100 MPa [25]. More recently, the same potential was demonstrated to give a quantitative account of the Joule–Thomson coefficient of methane at high pressure [21]. The exp-6 potential developed recently by Errington and coworkers [26] would have been well adapted to the investigation of water solubilities [9] but the absence of similar exp-6 potential for H_2S would have made the investigation of related mixtures difficult. As a result, it was decided to use Möller's potential for methane.

H_2S

In the present study we have used the potential proposed for H_2S by Kristof and Liszi [27] which involves a single Lennard–Jones 6–12 site and four electrostatic point charges. The parameters of the model are recalled in Table I. Simulations were made with numerical conditions similar to those used by Kristof and Liszi. A total number of 512 molecules were used, and the electrostatic interactions were cut at half of the both length, without using Ewald summation. Typical simulation length was 12×10^6 Monte Carlo steps. The simulation results obtained in the Gibbs ensemble have been compared with experimental correlations of vapour pressure, vapourisation enthalpy and saturated liquid density (Fig. 2). We have thus reproduced the excellent agreement reported by Kristof and Liszi about the coexistence properties of H_2S. As shown in a recent work [11] the use of Ewald summation instead of the cutoff method would have caused only small differences on H_2S equilibrium properties. In fact, our results are closer to those of Vorholz *et al.* [11] than from Kristof and Liszi [27] as we find also a slight underestimation of vapour pressures (Fig. 2a) and slight overestimation of the vapourisation enthalpy above 300 K (Fig. 2b). This indicates that the use of Ewald summation in Ref. [11] might not be the only reason of the observed deviations with Kristof and Liszi.

Further tests were also made against high pressure density data taken from Goodwin [28]. As shown in Table II, a very good agreement is found, with deviations ranging from +0.1 to +0.8%.

Water

Several intermolecular potentials have been proposed to model water. The simpler model is the SPC potential, in which the three electrostatic charges are located on the atomic centers of the oxygen and hydrogen atoms. In order to get a more realistic representation of liquid water properties, it was proposed to shift the negative charge from the oxygen nucleus toward an intermediate axial position, yielding the TIP4P potential [29]. It is known that the TIP4P model represents better the coexistence curve of water than the SPC potential particularly for temperatures lower than 500 K [30]. Numerous alternative models have been proposed

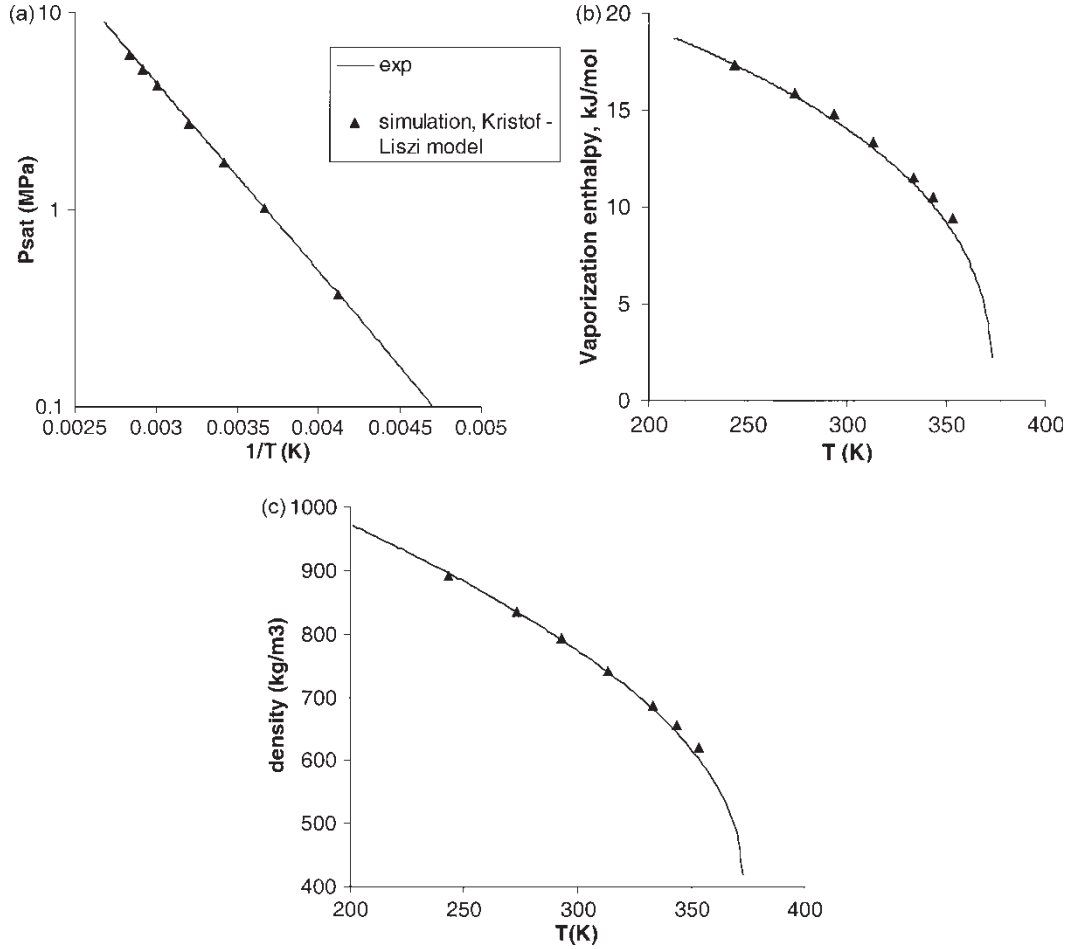

FIGURE 2 Gibbs ensemble simulation results for pure H_2S. Simulations based on the potential of Kristof and Liszi [27] are compared with experimental correlations from the Dortmund Data Bank (DDB). (a) Saturated vapour pressure, (b) vapourisation enthalpy, (c) saturated liquid density.

Downloaded At: 18:29 14 January 2011

since, involving either an exp-6 potential [9], polarisable models [31,32] or distributed electrostatic charges [33]. However, they would have been poorly compatible with the non-polarisable models selected for the other pure components. In addition, the consideration of polarisability does not seem sufficient to provide a significant improvement of coexistence properties, as illustrated by the attempt of Kiyohara *et al.* [32]. As a consequence, we privileged the TIP4P potential in our tests.

The TIP4P potential has been tested with two ways of evaluating the electrostatic energy: Ewald summation and a cut-off at 5, 7.5 or 10 Å. Cut-off values larger than 10 Å have not been tested because they would have violated the requirement that the cut-off must be lower than half the box length, which is slightly larger than 20 Å for the liquid in the conditions investigated here. When Ewald summation was used, preliminary tests were conducted to select suitable range parameters, i.e. $k_{max} = 7$ and $\alpha = 2\pi/L$, where L is box size. It was indeed recognised that different values of α were needed in the liquid and vapour phases to get an accurate calculation of energy. The coexistence properties were obtained by Gibbs ensemble simulations, using 300 molecules, with simulation lengths of 50×10^6

TABLE II H_2S density at high pressure obtained from simulation using the potential of Kristof and Liszi [27] compared with recommended values from Goodwin [28].

	T = 273 K			*T = 343 K*		
Pressure (MPa)	*Experiment*	*Simulation*	*Deviation (%)*	*Experiment*	*Simulation*	*Deviation (%)*
5	842.0	842.6	0.1	656.4	661.4	0.8
10.5	851.1	853.6	0.3	681.1	686.3	0.8
22.5	868.8	872.5	0.4	729.0	730.9	0.3
33	882.3	883.1	0.1	757.1	760.1	0.4
40	890.5	890.9	0.1	772.4	775.1	0.4

TABLE III Test of different ways to determine the electrostatic energy in the Gibbs ensemble simulation of water at 353 K (300 molecules, $50-105\times10^6$ MC steps). Subscripts indicate the estimated statistical uncertainty on the last digit.

Property	*Ewald*	*Cutoff*		
		5 Å	*7.5 Å*	*10 Å*
P_{sat} (kPa)	64_5	58_6	65_3	61_3
ρ_{liq} (kg/m^3)	957_4	1006_4	971_4	955_3
ΔH_{vap} (kJ/mol)	40.9_2	43.3_2	41.5_1	40.9_1

Monte Carlo steps at least. These long simulations were indeed necessary to obtain reasonably consistent results. As can be seen from the results shown in Table III, the saturated vapour pressure, the vapourisation enthalpy and the liquid density computed with a cutoff of 10 Å agree with Ewald summation almost within the estimated statistical uncertainties. Larger deviations are logically found with cut-off values of 7.5 and 5 Å, which overestimate density and cohesive energy.

The trend of saturated vapour pressure of water between 273 and 373 K appears similar with a 10 Å cutoff and with Ewald summation, indicating an overestimation of this property (Fig. 3). These results are in very good agreement with previous results obtained with the TIP4P potential [34,35]. As the TIP4P potential was optimised on the basis of simulations performed with a cut-off of electrostatic interactions at 7.5 Å [29] and did not consider vapour pressure, it is not surprising that such systematic differences are found. Similar comparisons have been made for vapourisation enthalpy, indicating deviations between +1.4 kJ/mol at 273 K and −1.0 kJ/mol at 373 K, while the statistical uncertainty is approximately 0.2 kJ/mol. The deviations on liquid density were found to range between +10 kg/m^3 at 273 K and −24 kg/m^3 at 373 K. Both properties are well described, but their variation with temperature is exaggerated compared with experimental observations. Here again, these results are identical to previous simulation results [34].

In the following simulations, the electrostatic energy has been evaluated with the cut-off method only. This option presents the practical advantage that it requires approximately four times less computer time than Ewald summation. For a given computing time, the use of a 10 Å cutoff allows much longer simulations and thus provides much better convergence of thermodynamic averages. However, care has to be taken that the results may depend significantly on numerical parameters [36]. In order to limit this effect, we decided to perform most following simulations with similar box sizes, i.e. 270–300 water molecules in the aqueous liquid box.

CO_2

CO_2 was simulated first with the rigid version of the EPM2 intermolecular potential of Harris and Yung [37] and with the two-centres + quadrupole model of Vrabec *et al.* [38]. While testing these models, we used only the cut-off method to evaluate the electrostatic energy. The simulations were conducted with 400 molecules over 30×10^6 steps, using the cutoff method to compute the electrostatic interactions. In the case of the Vrabec model, the point quadrupole was simulated as a set of three point charges placed on the molecular axis at ±0.5 Å from the carbon nucleus (Table I) in order to match the quadrupole moment of the molecule, which is 4.3×10^{-40} C m^2 [39].

These intermolecular potentials have been tested at four different state points. The first two state points corresponded to the vapour–liquid equilibrium at 216.6 K, i.e. at the triple point, and at 270 K, i.e. closer to the critical temperature which is 304.1 K. These conditions allow us to check the representation

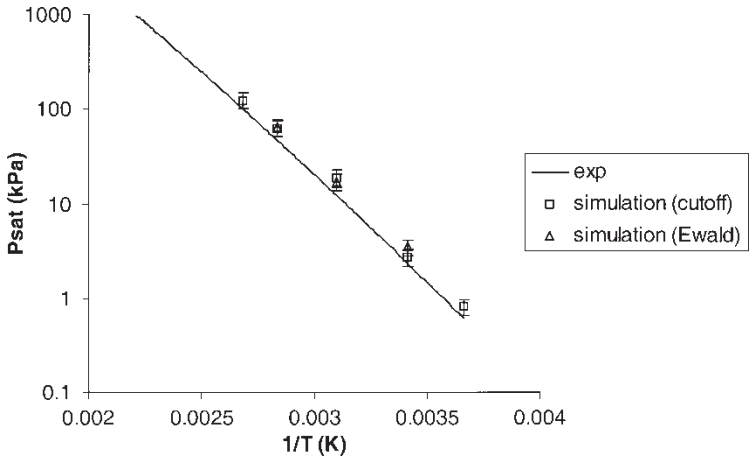

FIGURE 3 Saturated vapour pressure computed with the Gibbs ensemble method for pure water based on the TIP4P potential. Simulations performed with Ewald summation and with a 10 Å cutoff of the electrostatic interactions are compared with experimental correlations from the Dortmund Data Bank (DDB).

Downloaded At: 18:29 14 January 2011

TABLE IV Comparison of pure CO_2 simulation results with the EPM2 rigid CO_2 model of Harris and Yung [37], the potential of Vrabec *et al.* [38] and the potential slightly reparametrised in this work (EPM-W) at five state points.

			EPM2 [37]		*Vrabec et al.*		*EPM-W*	
		Experiment	*MC simulation*	*Deviation (%)*	*MC simulation*	*Deviation (%)*	*MC simulation*	*Deviation (%)*
216.6 K	P_{sat} (MPa)	0.518	0.592	14	0.569	9.8	0.485	6.4
	ΔH_{vap} (kJ/mol)	15.15	15.05	0.7	15.49	2.2	15.96	5.3
	ρ (kg/m^3)	1178	1165	1.2	1158	1.8	1184	0.4
270 K	P_{sat} (MPa)	3.203	3.65	14	3.38	5.5	3.04	5
	ΔH_{vap} (kJ/mol)	10.56	10.28	2.7	10.64	0.7	11.37	7.6
	ρ (kg/m^3)	946	936	1	919	3	962	1.6
370 K	ρ at $P = 7$ Mpa	122	118	3	118	3.3	120	1.7
	ρ at $P = 40$ MPa	767	–	–	–	–	764	0.4
	ρ at $P = 80$ MPa	940	924	1.8	903	4	935	0.5

of the coexistence properties with the Gibbs ensemble. The other state points were selected in the supercritical region ($T = 370$ K) at two pressure levels (7 and 80 MPa). Their role is to test the volumetric behaviour of CO_2 in representative conditions of possible CO_2 reinjection, using monophasic NPT simulations.

The results of these tests are shown in Table IV. The Harris and Yung potential predicts densities and vapourisation enthalpies within 3%. High densities, either in the liquid state at 216 and 270 K or in the supercritical region at high pressure, are predicted with an accuracy better than 2%. This satisfactory result confirms previous findings with the EPM2 model [34,35,40]. However, saturated vapour pressures are overestimated by 14%. This result confirms the slight overestimation of vapour pressures found in previous works using the EPM2 model of Harris and Yung [34,35].

The Vrabec potential predicts saturated vapour pressures with a better precision (10%), but the deviations on densities reach 4% at high temperature and high pressure.

Considering that either potential had its merits and flaws, we have attempted to optimize further the parameters of the Harris–Yung potential, using the optimization method recently proposed by Bourasseau *et al.* [41]. This consisted in defining a least squares error criterion on the basis of the experimental measurements indicated in Table IV, including thus the two supercritical fluid densities as an additional reference data. The error criterion was minimised to get the optimum Lennard–Jones parameters, using the EPM model of Harris and Yung as a starting point. However, we decided to set the C—O distance to the recommended value of 1.16 Å [42]. Two parameters may be optimized per atom, i.e. four altogether. It was found that optimizing three or four parameters resulted in important variations from the EPM parameters, indicating that the optimization was poorly stable. This may be attributed to an insufficient amount of independent information in the error criterion compared with the number of optimized parameters, as discussed by Bourasseau *et al.* When optimization was restricted to the two Lennard–Jones parameters of the oxygen, a significant improvement of supercritical density prediction was obtained with a very small variation of these parameters: ε and σ are changed by less than 1 and 0.1%, respectively, from the original EPM model, indicating that the optimisation is likely to preserve most of its physical basis (Table I). As shown in Table IV, densities are predicted within 1.7% and saturated vapour pressures within 7% for the reference state points. However, the vapourisation enthalpies are less accurately predicted, since errors may reach 7.6%. Nevertheless, it was estimated that the optimised model EPM-W was a better compromise, as density prediction is important for our purpose.

PHASE EQUILIBRIA IN THE WATER–METHANE–H_2S SYSTEM

Methane–H_2S System

The methane–H_2S system has been investigated in the Gibbs ensemble at imposed pressure for three temperatures: 223, 273 and 343 K. The total number of molecules was 600–800, and the length of the simulations was $1–3 \times 10^7$ steps. As a general feature, convergence was more difficult for the high pressures in a given phase diagram, and density exchange between phases was observed when getting close to the critical point. At the lower temperature of 223 K, the bubble pressures appear again to be somewhat underestimated, but the dew points are well represented (Fig. 4a). We also investigated higher pressures than those shown on Fig. 4a, looking for possible liquid–liquid equilibrium at high pressure as suggested by experimental data [6,7]. Although the system showed some tendency to stay as two separate phases in these conditions, convergence was very slow and we preferred not to trace the simulated phase diagram above 10 MPa.

Downloaded At: 18:29 14 January 2011

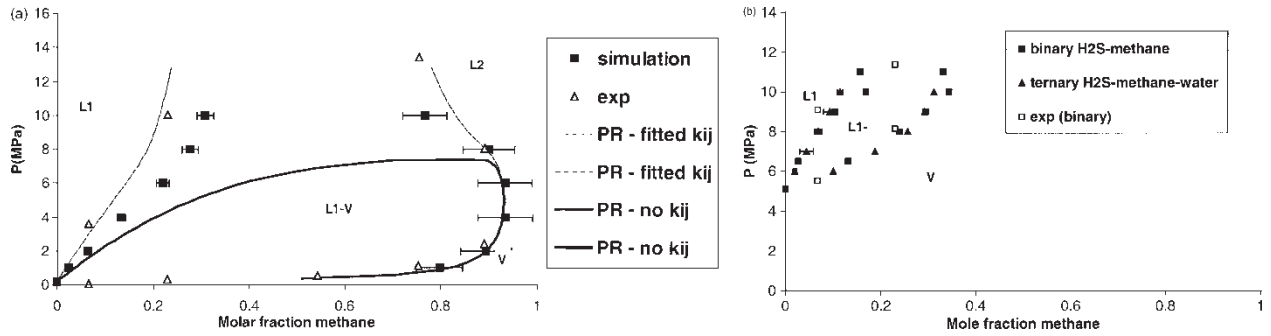

FIGURE 4 Phase equilibrium simulation of the methane–H_2S binary system at 223 K (a) and 343 K (b), compared with interpolated data points of Kohn and Kurata [6,7] and with the predictions of the Peng–Robinson cubic equation of state (PR).

Compared with a classical cubic equation of state [43] without interaction parameters, molecular simulation results are significantly better. However, tuning of a binary interaction parameter on the experimental phase diagram makes the cubic equation of state more precise than simulation.

At 343 K, the phase diagram is reasonably predicted (Fig. 4b). A similar agreement is found at 273 K (not shown).

Methane–water System

The phase behaviour of the methane–water system was investigated in the Gibbs ensemble at imposed pressure, as no three-phase equilibrium is suspected. A total number of 500 water molecules and 200 methane molecules were used in these simulations. The higher number of water molecules was aiming at avoiding excessively low mole numbers of methane in the aqueous phase, due to the low solubility. The cut-off distance, which is common to the Lennard–Jones and electrostatic interactions, was set to 10 Å in order to keep approximately the same way of evaluating energy as in the study of pure water. The simulated solubility of methane in the water phase, shown in Fig. 5a, shows that the solubility of methane is underestimated by approximately 30% at high pressure. This deviation may seem quite high but it is in fact similar to the deviations found with other potentials when computing Henry's constants [8,9]. We can notice that the apparent Henry's constant (P/x) is increasing with increasing pressure, as observed in Refs. [3,44]. The decrease of water solubility in the methane–rich vapour phase with increasing pressure is well reproduced, as shown by Fig. 5b.

Water–H_2S System

In the 273–373 K range, the H_2S–water system is known to exhibit liquid–vapour equilibrium at low pressure and liquid–liquid equilibrium at high pressure [4], both domains being connected with a three-phase equilibrium line. This system was tested at 343 K (Fig. 6), using either Gibbs ensemble at imposed pressure for two-phase conditions or the Gibbs ensemble at imposed volume for three-phase calculations. The simulated system comprised approximately 300 water molecules and 500 H_2S molecules. A $30–55 \times 10^6$ MC steps were found sufficient to provide a satisfactory convergence of simulation averages. When analysing typical configurations of the H_2S-rich liquid phase, we observed that the water molecules are organised in clusters which were found to contain up to four molecules, while such a self-association of water is not found in the vapour phase. In order to test the sensitivity of this association to system size, we repeated the simulations with 900 H_2S molecules instead of 500, so that the H_2S-rich liquid contains a more

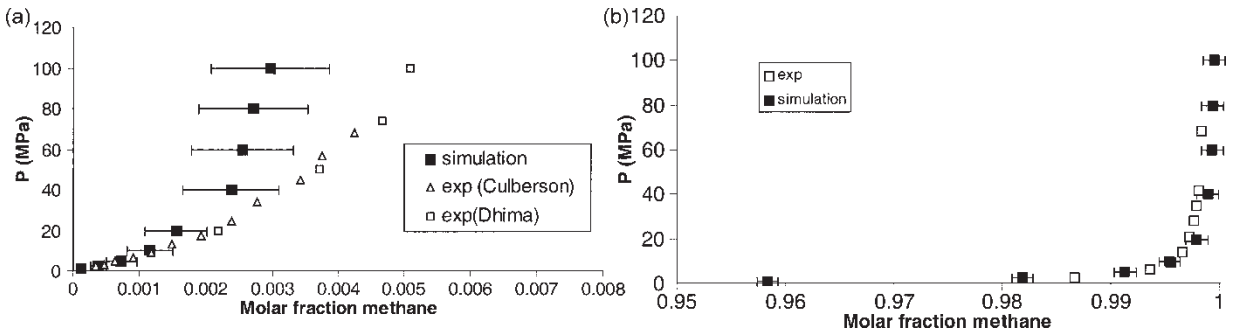

FIGURE 5 (P, x) phase diagram of the methane–water binary system at 343 K. (a) Solubility of methane in the aqueous phase. (b) Composition of the vapour phase.

Downloaded At: 18:29 14 January 2011

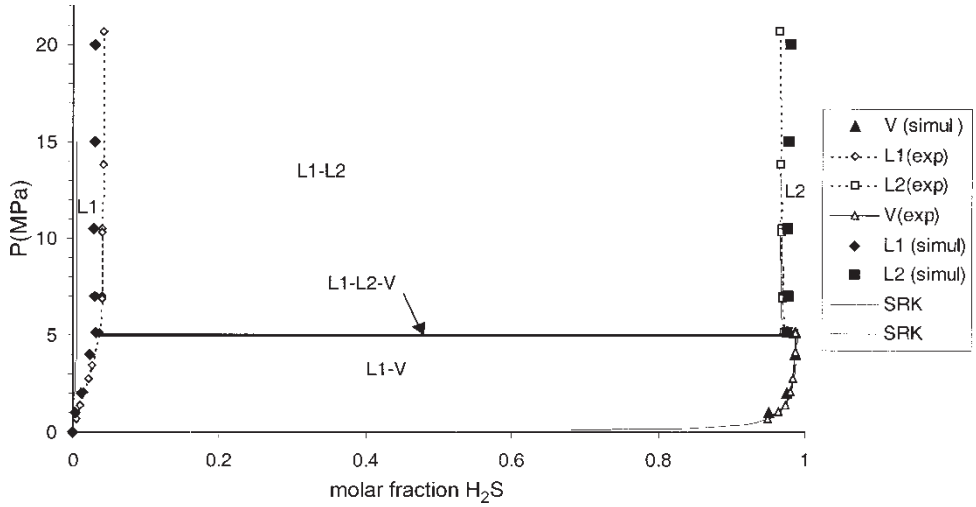

FIGURE 6 (P, x) phase diagram of the water–H_2S binary system at 343 K compared with experimental phase equilibrium data [4] and with the predictions of the Soave–Redlich–Kwong cubic equation of state (SRK).

representative number of water clusters. In order to study water clustering, we performed a preliminary cluster analysis on the basis of a simplified criterion (centre-to-centre distance lower than 3.5 Å, i.e. 1.15 times the Lennard–Jones diameter of water). The resulting cluster size distribution, based on the analysis of 12 different configurations (Fig. 7) shows that clusters of two, three and four water molecules are found with significant amounts. The total number of such clusters is approximately 20% of the number of monomers. When the distribution is expressed on a mass basis, as logical for polydisperse systems, we see that 40% of the water molecules are found in clusters. When changing from 500 to 900 molecules in the H_2S-rich liquid phase, we also observed an increase of the water solubility in liquid H_2S. When this phase is represented by a total of 500 molecules, the average number of water molecules is less than 10. This small number is responsible for an incomplete sampling of the cluster size distribution. We therefore decided to perform further simulations with approximately 900 molecules in this phase.

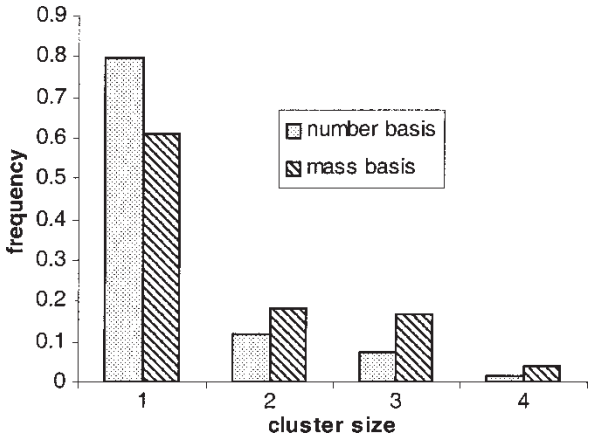

FIGURE 7 Cluster size analysis of the water clusters in the H_2S-rich liquid phase in equilibrium with a vapour phase and an aqueous phase at 343 K. The number basis distribution expresses the percentage of clusters of a given size, while the mass basis distribution shows the percentage of water molecules belonging to clusters of a given size.

The prediction of the whole phase diagram is satisfactory, since the liquid–liquid and liquid vapour domains are found as expected. The three-phase equilibrium pressure determined from the three-phase Gibbs ensemble calculation at imposed volume is in very good agreement with the observed behavior. Simulation results predict qualitatively the higher solubility of water in the H_2S-rich liquid phase (approximately 3%) than in the vapour phase (approximately 1.3%). These results are in general agreement with a previous investigation of the water–H_2S system with the same potential by Vorholz *et al.* [11] who found also a liquid–liquid phase split at high pressure but did not determine explicitly the L–L–V three phase equilibrium line. The solubility of H_2S in the aqueous phase below the three-phase equilibrium pressure is in good agreement with Vorholz *et al.* However, it is likely that the insufficient size of the H_2S-rich liquid box in their study explains why they found a smaller water content in the H_2S-rich liquid phase at high pressure.

The tests we have performed with the Soave–Redlich–Kwong equation of state [45] indicate that the water–H_2S phase diagram cannot be reproduced, even qualitatively, if no binary parameter is fitted for this purpose. When fitting a binary parameter on the H_2S–water equilibrium data, the water solubility in H_2S can be reproduced correctly, but not the solubility of H_2S in water which predicted lower than 1% (Fig. 6). In order to represent the phase diagram with a common model for both phases, we had to use a more advanced equation of state using a mixing rule based on an excess Gibbs energy model [46].

Downloaded At: 18:29 14 January 2011

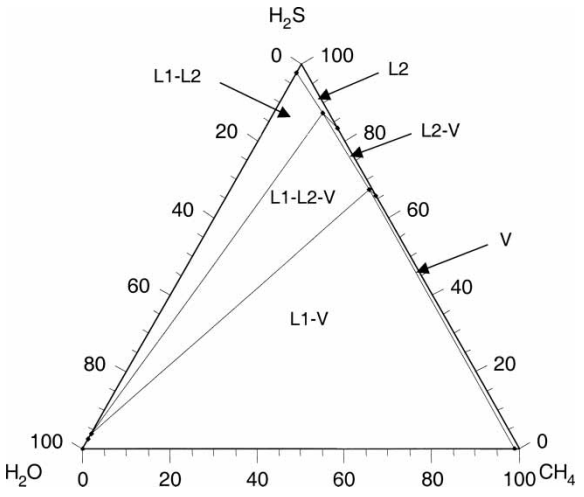

FIGURE 8 Ternary phase diagram of the water–H_2S–methane system at 343 K at 10 MPa.

Water–Methane–H_2S Ternary System

The behaviour of the ternary system has been investigated with three-phase and two-phase Gibbs ensemble calculations at imposed temperature and pressure. At imposed pressure and temperature, the three-phase conditions correspond to coexisting phases with identical composition, whatever the global composition of the system. Thus a single three-phase simulation is sufficient to trace the end-points and boundaries of the three-phase diagram. Selected results obtained at 343 K and 10 MPa are shown in the ternary diagram of Fig. 8. From this graph, it can be seen that the composition of the vapour phase and of the non-aqueous liquid phases are little affected by the presence of water. Indeed, the water content is small in these phases. When the H_2S-rich liquid phase is diluted with methane, the solubility of water drops rapidly. For instance, the solubility of water in a mixture of 80% H_2S and 20% methane is only one third to one half of the solubility of water in pure H_2S (Fig. 9).

VOLUMETRIC AND ENTHALPIC PROPERTIES OF THE H_2S–CO_2 SYSTEM

Test of Combining Rules

In order to test the capability of molecular simulation to provide accurate density predictions for H_2S–CO_2 mixtures, comparisons have been made with the experimental measurements provided by the GPA [47]. These measurements have been performed for H_2S concentrations up to 50% and pressures up to 23 MPa, at temperatures between 200 and 450 K. Our tests have been conducted along three isotherms (273, 350 and 400 K), within the pressure and composition range where data were available for these isotherms. They comprised 23 state points, covering low density regions as well as high density regions.

The first tests were performed with the Lorentz–Berthelot combining rules. At 273 K, we recorded deviations up to 10.1% on the liquid density of the equimolar H_2S–CO_2 mixture. At 350 K, a maximum deviation of 126% was found on the density of the equimolar mixture at 10 MPa. The prediction at 400 K showed deviations lower than 1.2% with experimental measurements. The maximum deviations at 273 and 350 K are extremely disappointing, since the pure component densities were predicted within 2–3%. However, it may be noticed that the most important deviations at 350 K are limited to a specific part of the supercritical region where system density is extremely sensitive to small changes of pressure,

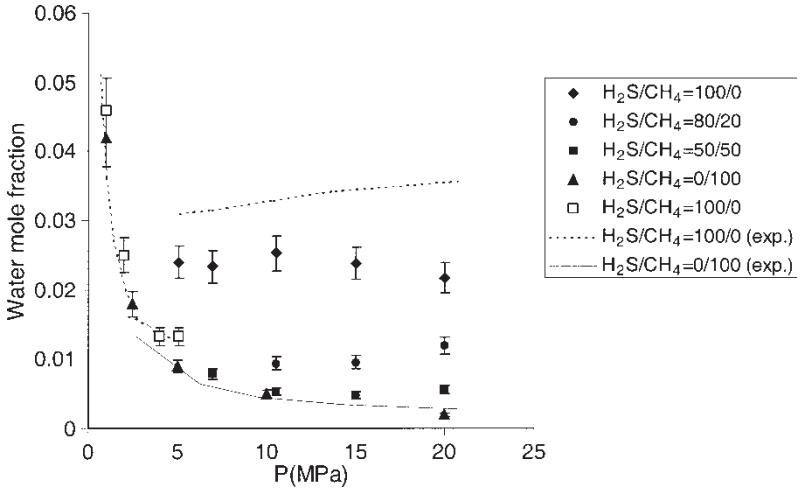

FIGURE 9 Solubility of water in H_2S or methane-rich phases at 343 K as a function of pressure. The full lines represent the experimental solubility in the water–methane system and dotted lines in the H_2S system [4]. Open symbols refer to solubilities in the vapour phase in the H_2S–water binary system, below the three-phase equilibrium pressure of 5.1 MPa. Full symbols refer to the solubility in dense phases at higher pressures, with various H_2S–methane ratios in the ternary system.

Downloaded At: 18:29 14 January 2011

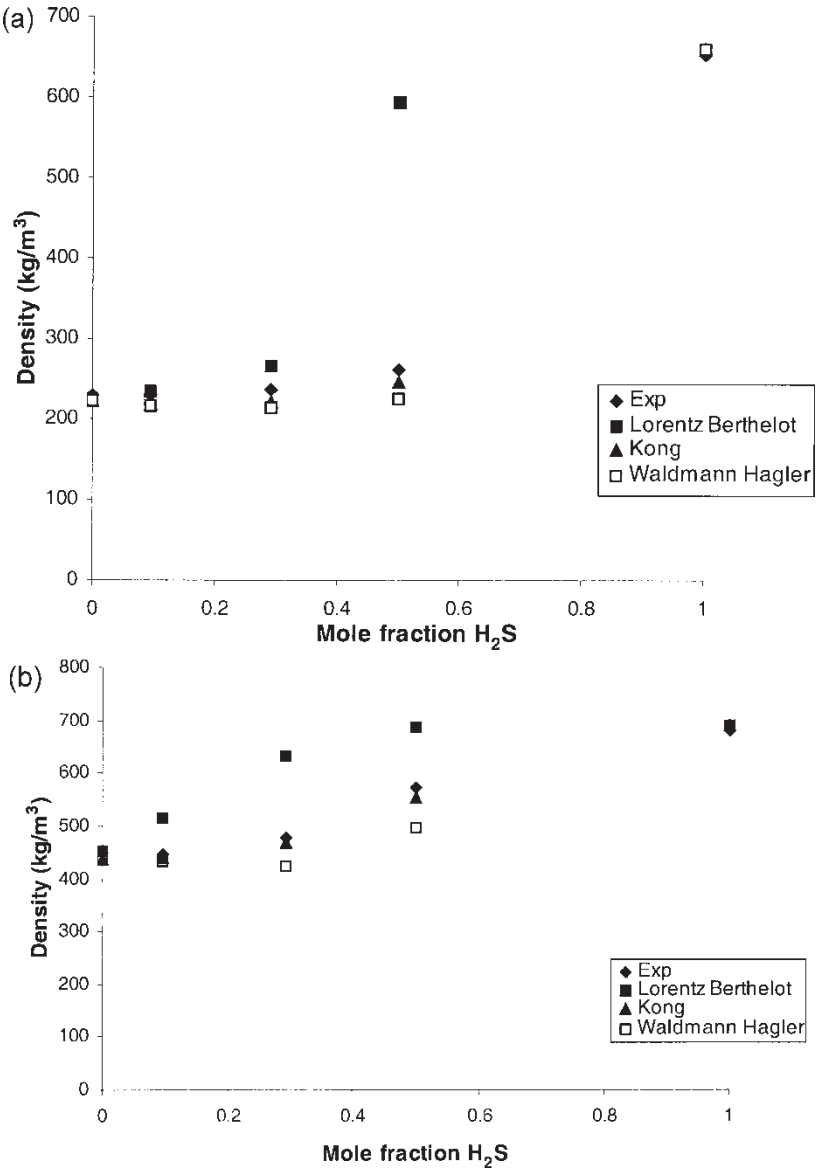

FIGURE 10 Prediction of the density of the H_2S–CO_2 system with various combining rules at 350 K as a function of composition (a) 10 MPa, (b) 15 MPa. The experimental data are taken from Kellermann *et al.* [47].

temperature or composition. Also, it may be recalled that density predictions in this region are difficult with equations of state.

In order to improve prediction without fitting additional model parameters, it was decided to test alternate combining rules. Indeed, it has been reported that alternate combining rules (Kong or Waldmann–Hagler) yield better prediction of liquid–vapour phase equilibria [15,19]. This is particularly the case when the atoms (or united atoms) involved in the mixture differ significantly in diameter. Indeed, the Kong and Waldmann–Hagler mixing rules are based on a geometric mean on the attraction term $\varepsilon\sigma^6$ rather than on the Lennard–Jones parameter ε. In our case, the main interaction between H_2S and CO_2 originates from the oxygen–H_2S interaction, involving groups of 3.0356 and 3.73 Å. This significant size difference announces a likely influence of the combining rules.

Indeed, the replacement of the Lorentz–Berthelot by the Kong or Waldmann–Hagler mixing rules produces very significant changes concerning density predictions. As illustrated by Figs. 10a and b which correspond to the most problematic conditions with the Lorentz–Berthelot rules, the alternate combining rules provide a much more satisfactory prediction of mixture densities in this region. As shown in Table V, the alternate combining rules also provide improved prediction of liquid density at 273 K, since the maximum deviations are 1.3% (Kong) and 1.9% (Waldmann–Hagler). The densities at 400 K are not predicted as well as with Lorentz–Berthelot, since maximum deviations of 3.1% (Kong) and 4.2% (Waldmann–Hagler) were

Downloaded At: 18:29 14 January 2011

TABLE V Influence of the combining rule on the density of H_2S–CO_2 mixtures in the liquid state at 273 K, compared with experimental measurements [47].

Molar fraction of H_2S	*Pressure (MPa)*	*ρ_{exp} (kg/m^3)*	*Lorentz–Berthelot*		*Kong*		*Waldmann–Hagler*	
			$\rho_{simulation}$	*% Δ*	*$\rho_{simulation}$*	*% Δ*	*$\rho_{simulation}$*	*% Δ*
0.0955	15	951.9	1003.1	+5.4	964.5	+1.3	956.0	+0.4
0.2933	15	913.8	987.6	+8.1	926.0	+1.3	902.7	−1.2
0.500	2.7	846	931.4	+10.1	853.8	+0.9	829.7	−1.9

found, as illustrated by Table VI. As a whole, the Kong combining rules appear clearly as the best possible choice for the H_2S–CO_2 system.

A potential problem when changing the combining rules is that they may change the properties of pure CO_2, since the carbon–oxygen interaction plays a role in pure component properties and the combining rules influence its parameters. We have tested this point by computing again the coexistence curve and supercritical densities of CO_2 with the EPM-W potential parameters and the Kong combining rules. The maximum deviations on saturated liquid densities, vapourisation enthalpies and saturation pressures were found to be significantly smaller with the Kong combining rules than with the Lorentz–Berthelot. The supercritical densities of CO_2 were predicted with a maximum deviation of 3.3%, a slightly worse prediction than the 2.5% maximum deviation which was encountered with the Lorentz–Berthelot combining rules. As a whole, it may be concluded from this test that the properties of pure fluid CO_2 are still represented with a very good accuracy when the Kong combining rules are used with the optimised parameter set EPM-W.

Downloaded At: 18:29 14 January 2011

Prediction of Densities and Excess Volumes at High Pressure

As established in the previous section, the Kong combining rules offer the best prediction of mixture densities in the H_2S–CO_2 system for a large range of test conditions, either in the vapour, liquid or supercritical state. It was thus decided to use molecular simulation to provide reference predictions for the same system at high pressure, where no experimental data are presently available. These reference predictions aim at capturing the influence of pressure, temperature and composition. We investigated all the possible combinations involving four temperatures (273, 323, 373 and 423 K), four pressures (20, 40, 60 and 80 MPa) and five mole fractions (0, 25, 50, 75 and 100% H_2S). Thus 80 simulations were performed.

The densities obtained at 323 and 423 K are shown in Fig. 11a and b. Among others, these graphs show that the influence of composition changes significantly in the high-pressure range. For instance, an increase of H_2S molar fraction at 423 K causes an increase in density at 20 MPa while it causes a decrease of density at 80 MPa. The volumetric properties of the H_2S–CO_2 system have also been investigated for the same state points, using a modified version of the Benedict–Webb–Rubin equation of state [48]. The densities predicted by this route are in fair agreement with molecular simulation results, as the maximum differences are approximately 3% over all state points investigated. This equation of state seems to predict slightly lower densities for intermediate molar fractions (25–75%), however. From these results, it was also possible to compute excess volumes. The statistical uncertainty in the determination of excess volumes is estimated to be 0.5–1 cm^3/mol depending on conditions. As a general feature, excess volumes are positive in the investigated range of conditions, and their evolution with H_2S molar fraction is approximately parabolic, as illustrated by Fig. 12. At 273 and 323 K, the pure components are both displaying liquid-like densities in the whole pressure range, and excess volumes are found to be small (typically 2 cm^3/mol or less). Higher excess volumes are found at

TABLE VI Influence of the combining rule on the density of H_2S–CO_2 mixtures 400 K, compared with experimental measurements [47].

Molar fraction of H_2S	*Pressure (MPa)*	*$\rho_{experiment}$ (kg/m^3)*	*Lorentz–Berthelot*		*Kong*		*Waldmann–Hagler*	
			$\rho_{simulation}$	*% Δ*	*$\rho_{simulation}$*	*% Δ*	*$\rho_{simulation}$*	*% Δ*
0.0955	5	71.9	71.3	−0.8	71	−1.5	70.7	−1.6
	7.5	113.9	113	−1.1	111.2	−2.3	110.8	−2.7
0.2933	5	69.6	69	−0.7	68.2	−1.9	67.5	−3
	7.5	111.0	110	−0.8	107.5	−3.1	107	−3.5
0.500	5	67.5	67	−1.1	65.5	−2.9	65.2	−3.4
	7.5	107.9	109	+1.2	105	−2.8	103.4	−4.2

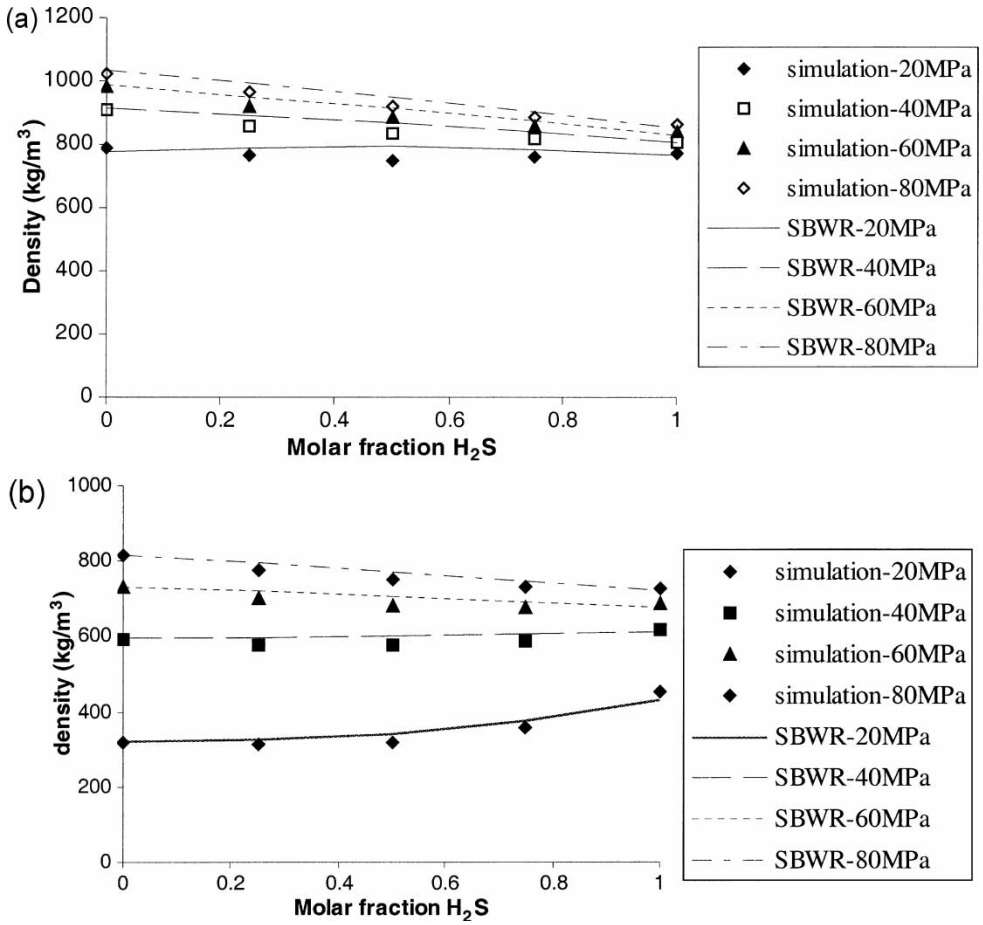

FIGURE 11 Density prediction of H_2S–CO_2 system as a function of composition and pressure by molecular simulation using the Kong combining rule at 323 K (a) and 423 K (b) SBWR refers to the predictions of the non-cubic equation of state of Soave [48].

Downloaded At: 18:29 14 January 2011

373 and 423 K, particularly at 20 MPa, where they exceed 10 cm^3/mol.

Prediction of Excess Enthalpies

The statistical uncertainty on excess enthalpy, determined from Eq. (5), has been found to be approximately 100 J/mol. Excess enthalpies are readily obtained for the same set of conditions as excess volumes (pressures of 20–80 MPa, temperatures 273–423 K and compositions of 0, 25, 50, 75 and 100% H_2S). As a general rule, the excess enthalpies in the H_2S–CO_2 system are found to parallel the behaviour of the excess volumes. Indeed, excess enthalpy also

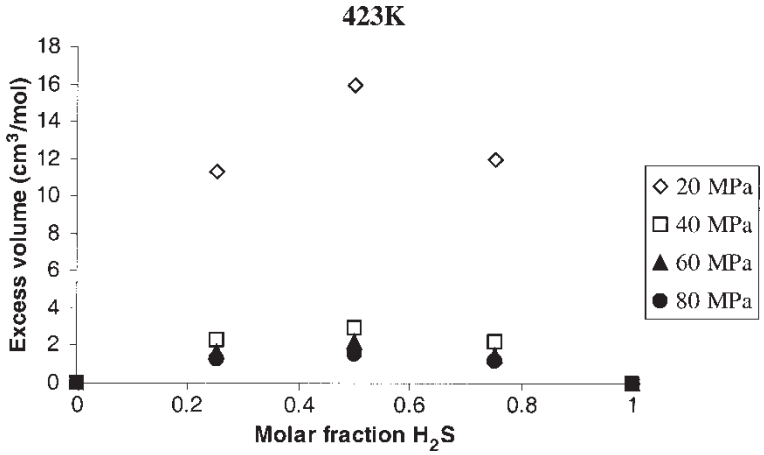

FIGURE 12 Molar excess volume in the H_2S–CO_2 system as a function of composition and pressure at 423 K, predicted with the Kong combining rule.

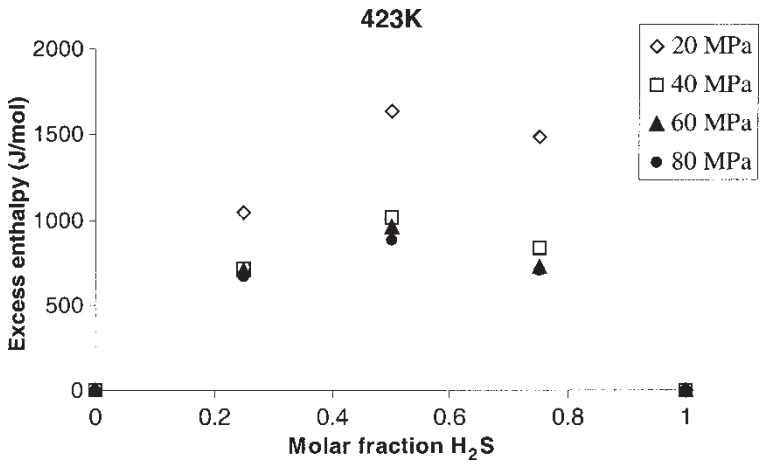

FIGURE 13 Molar excess enthalpy in the H_2S–CO_2 system as a function of composition and pressure at 423 K, predicted with the Kong combining rule.

showed a parabolic dependence with composition. The amplitude of excess enthalpies is also found higher at the lower pressure (20 MPa) and the higher temperature (423 K) of the investigated range (Fig. 13).

Prediction of Derivative Properties

In Table VII, we show the predictions of heat capacity, isobaric thermal expansion coefficient, isothermal compressivity and Joule–Thomson coefficient of pure CO_2 and pure H_2S in test conditions (350 K) where CO_2 is supercritical while H_2S is subcritical. It may be seen that the first three properties are predicted with a maximum deviation of 13%. The prediction of the Joule–Thomson coefficient appears less accurate, since deviations reach 30%. In fact the statistical uncertainty on the Joule–Thomson coefficient is estimated to be approximately $0.1\,K.MPa^{-1}$, so that the predicted values are in reasonable agreement with experimentally-based values if the uncertainty is considered. The inversion of the Joule–Thomson coefficient when changing from H_2S to CO_2 is well described.

DISCUSSION

From a process engineering standpoint, the general question raised by molecular simulation methods is whether they may provide contributions that would be impossible or difficult to obtain with experimental measurements and/or classical thermodynamic models. In the present study, we can reformulate the question as "is it worth doing such lengthy calculations to predict properties of H_2S-rich systems"?

A first way of answering the question is to examine the capability of molecular simulation algorithms to compute the desired thermodynamic properties within a reasonable computer time. In the present study, various properties were addressed: molar volume, thermodynamic derivative properties (heat capacity, compressibility,...), excess volumes, excess enthalpy, and phase equilibria (either with two or three coexisting phases). In a few cases, we felt some limitations of the implemented algorithms because of slow convergence (for instance aqueous phases at ambient temperature) or because of low solubility. Very low solubilities, as encountered in the water–methane system at low pressure for instance, could be addressed in future studies through appropriate Widom tests [49]. Also, we have experienced a well-known limitation of the Gibbs ensemble technique to perform phase equilibrium calculations in the vicinity of the critical region. In the target range of pressure and temperature, this holds for pure compounds (such as H_2S) as well as for mixtures (such as methane–H_2S, see Fig. 4b). In order to investigate the critical region, the histogram reweighting technique [15] would probably provide a very efficient improvement. An original point

TABLE VII Comparison of thermodynamic derivative properties of pure H_2S and pure CO_2 at 350 K and 40 MPa. Experimental data are from the IUPAC correlation [51] in the case of CO_2 and from Goodwin [28] in the case of H_2S.

	H_2S			CO_2		
	Experiment	*Simulation*	*Deviation*	*Experiment*	*Simulation*	*Deviation*
Heat capacity ($J\,mol^{-1}\,K^{-1}$)	61.62	66.7	+8.3%	81.3	79.2	−3.8%
Isobaric thermal expansion coefficient ($K^{-1} \times 10^{-3}$)	2.43	2.34	−3.7%	4.03	3.66	−9.2%
Isothermal compressibility (kPa^{-1})	2.88	2.77	−3.8%	7.27	6.30	−13.3%
Joule–Thomson coefficient ($K.MPa^{-1}$)	−0.109	−0.148	−36%	0.266	0.191	−28%

Downloaded At: 18:29 14 January 2011

in our study has been the investigation of excess enthalpy and excess volume. Although these properties are determined with a significant statistical uncertainty, the major trends can be identified without any problem.

Nevertheless, we have not encountered serious limitations because of the available algorithms in the present study. All the results have been obtained with a few PC-Linux workstations, so the computer cost is a minor part in the molecular simulation study compared with manpower. A factor that eased the study significantly was the implementation of the various algorithms (NPT, Gibbs ensemble, fluctuations) in a consistent software package, so that the time spent in file checking and data processing was reasonable. However, substantial improvements are still expected from more powerful computers and improved algorithms.

A second way to evaluate our study is to discuss prediction capability from a qualitative standpoint. In this respect, we have to stress first that the intermolecular potentials used in the present investigation have been determined from pure component parameters only. Despite this disadvantage, molecular simulation results agree generally well with available experimental results on the phase equilibrium of binary mixtures. This is not very surprising for the methane–H_2S system, since it is known that the phase behavior of alkane–H_2S systems is correctly predicted with standard potentials [40]. Nor is it surprising that fair predictions are found for the water–methane binary mixture, as this system is reasonably described with simple potentials [8–10]. The case of the water–H_2S mixture is more interesting, since molecular simulation predicts the liquid–liquid immiscibility at high pressure as well as the three-phase equilibrium conditions. It is particularly satisfactory that the solubility of water is found larger in the H_2S-rich liquid than in the vapour phase, in agreement with experimental measurements and earlier simulations [11]. According to our simulations, this phenomenon is probably due to the association of water in small clusters in the H_2S-rich liquid phase, resulting from the strong dipole moment of water molecules. The number-based distribution shown in Fig. 7 is not very far from the exponentially decreasing distribution that is found with classical association models when the Gibbs energy of association is considered constant per molecule. Two facts indicate that this distribution is clearly non-random. The first is that the probability for a water molecule to be in a monomer is 60%, while it would be approximately 80% in a random liquid containing 2% of water molecules. The second fact is the importance of trimers, which would be almost negligible in a random fluid. However, we must keep in mind that the cluster analysis is preliminary. In future studies, a more appropriate definition of the clusters should be made on the basis of the hydrogen–oxygen distance [50].

We may notice that the usual procedure to determine Henry's constants from biased Widom tests [8,9] would not have been adapted to determine the solubility of water in the H_2S-rich liquid phase. Indeed, this procedure would have measured the solubility of the monomers only, and it would not have accounted for the association of water in small clusters.

Regarding single phase properties like densities or derivative properties, predictions are also satisfactory. It is particularly encouraging that the change in sign of the Joule–Thomson coefficient is correctly predicted at high pressure when changing from CO_2 to H_2S.

The third point that we will discuss here is the capability of molecular simulation to provide quantitative results. With respect to the phase equilibria of binary systems, our results are not as accurate as state-of-the art thermodynamic models, but they do not benefit from the calibration on binary systems which has been performed with these models. Simulation might be of equivalent accuracy for the ternary system, for which no experimental data are available. For instance, the prediction of water solubility in the H_2S liquid phase as a function of the methane content (Fig. 9) is probably safer from molecular simulation, because of the self-association of water molecules in this process. With respect to volumetric properties, molecular simulation provides an equivalent accuracy to state-of the art equations of state for pure compounds as well as for the investigated mixtures, as illustrated by the H_2S–CO_2 system. In this case, the consistent comparison with the non-cubic equation of state of Soave [48] validates its use as an engineering equation of state in a fully independent way. It may be objected that obtaining good predictions has required a change of the combining rules, as the Lorentz–Berthelot usual prescription did not provide satisfactory answers for the binary CO_2–H_2S mixture. However, the Kong and Waldmann–Hagler combining rules have been already reported as being more satisfactory, from a theoretical as well as from a practical viewpoint [15,19]. They are indeed based on the geometric mean of the $\sigma^6\varepsilon$ coefficient, which is more defendable from the theory of the London dispersion forces than the geometric mean of the ε coefficient used in the Lorentz–Berthelot rules. In retrospect, it appears that we should repeat the whole study with Kong's combining rules. This would not require us to optimize again the Lennard–Jones parameters for methane, H_2S and water, as the properties of these pure components do not depend on the combining rules. However, the phase equilibrium calculations on binary mixtures are certainly influenced by the combining rules and this should be tested. These tests

Downloaded At: 18:29 14 January 2011

are beyond the scope of the present study but will certainly be interesting in future work.

CONCLUSION

From an industrial standpoint, these results provide a fair prediction of phase behaviour in general and a key understanding of water solubility behaviour in H_2S-rich gases. If no phase equilibrium data had been available on binary mixtures, phase equilibria would have been predicted in a way sufficient for a preliminary process design. The deviations on the composition of the coexisting phases ranged from 1 to 5% in most cases, which may be considered a good performance as the intermolecular potentials used in the study have been determined exclusively from pure component properties. This capability is specific to molecular simulation, since binary systems involving polar compounds cannot be predicted from classical thermodynamic models without binary data, even from a qualitative standpoint. In the water–methane–H_2S system investigated here, much is already known, but the same approach could be applied to systems involving poorly known components, where data are scarce. There are numerous secondary components in natural gas like COS, thiols, or organo-mercuric compounds, for which little or no experimental information is available about their phase equilibria when mixed with hydrocarbons, water and common chemicals.

Density predictions are also very useful for the purpose of acid gas reinjection in deep reservoirs. Compared with cubic equations of state, molecular simulation has the advantage of predicting more safely derivative properties such as thermal expansivity or compressibility coefficient. Satisfactory prediction has been found on the H_2S–CO_2 system, for which maximum deviations on density are approximately 3% over a large range of composition, pressure and temperature. This has been obtained without calibration of any binary parameter. The predictions can be extended to extreme conditions, where they have been used to validate an engineering equation of state. However, we have to recognize that the prediction of this system was based on Kong's combining rules, while the first prediction with the Lorentz–Berthelot rules was disappointing. This illustrates the fact that the combining rules are still a poorly tested point in intermolecular potentials, which deserve more thorough studies in the future.

Based on the present study, we can precisely define the role molecular simulation can have in industrial projects. It cannot pretend to replace equations of state, which remain necessary for the tremendous number of repeated calculations involved in process design or in multiphase fluid flow simulation of reservoirs. Neither can it replace experiments when high accuracy data are needed for process design. Nevertheless, Monte Carlo simulation methods and associated intermolecular potentials may be considered as viable tools providing a qualitative understanding of fluid structure together with a fair prediction of thermodynamic properties, especially useful when classical models are limited by the lack of experimental data at an early stage of process development.

Acknowledgements

This work has been made in cooperation with the Compu Total, whose contribution is gratefully acknowledged. Special thanks are due to Anne Boutin and to the many researchers of the Laboratory of Chemical Physics and IFP who contributed to algorithm implementation and code development. We thank the referees whose suggestions contributed to improve the quality of this article.

References

[1] Minkkinen, M., Benayoun, M., Bartel, M. (1994) "Procédé de pré-traitement d'un gaz naturel contenant de l'hydrogène sulfuré." Patent no. 93/15765, France.
[2] Lecomte, F. (2001) "Procédé de prétraitement d'un gaz naturel contenant des composés acides." Patent no. 01/06224, France.
[3] Culberson, O.L. (1951) "Phase equilibria in hydrocarbon–water systems. The solubility of methane in water at pressures to 10,000 psi", *AIME Petr. Trans.* **192**, 223–226.
[4] Gillespie, P.C. and Wilson, G.M. (1982) "Vapor–liquid and liquid–liquid equilibria: water–methane, water–carbon dioxide, water–hydrogen sulfide, water–*n*-pentane, water–methane–*n*-pentane", *Research Report RR 48* (Gas Processors Association, Tulsa).
[5] Carroll, J.J. and Mather, A. (1989) "Phase equilibrium in the system water–hydrogen sulphide: experimental determination of the LLV locus", *Can. J. Chem. Eng.* **67**, 468.
[6] Kohn, J.P. and Kurata, F. (1959) "Volumetric behavior of the methane–hydrogen sulfide system at low temperatures and high pressures", *J. Chem. Eng. Data* **4**, 33–36.
[7] Kohn, J.P. and Kurata, F. (1959) "Heterogeneous phase equilibria of the methane–hydrogen sulfide system", *AIChE J.* **4**, 211.
[8] Economou, I. (2001) "Monte Carlo simulation of phase equilibria of aqueous systems", *Fluid Phase Equilibria* **183–184**, 259–269.
[9] Errington, J.R., Boulougouris, G.C., Economou, I.G., Panagiotopoulos, A.Z. and Theodorou, D.N. (1998) "Molecular simulation of phase equilibria for water–methane and water–ethane mixtures", *J. Phys. Chem. B* **102**, 8865.
[10] Errington, J.R., Boulougouris, G.C., Economou, I.G., Panagiotopoulos, A.Z. and Theodorou, D.N. (2000) "Molecular simulation of phase equilibria for water–*n*-butane and water–*n*-hexane mixtures", *J. Phys. Chem. B* **104**, 4958.
[11] Vorholz, J., Rumpf, B. and Maurer, G. (2002) "Prediction of the vapor–liquid phase equilibrium of hydrogen sulfide, and the binary system water–hydrogen sulfide by molecular simulation", *Phys. Chem. Chem. Phys.* **4**, 4449.
[12] Panagiotopoulos, A.Z. (1987) "Direct determination of phase coexistence properties of fluids by Monte Carlo simulation in a new ensemble", *Mol. Phys.* **61**, 813–826.
[13] Allen, M.P. and Tildesley, D.J. (1987) *Computer Simulation of Liquids* (Oxford Science Publications, Oxford).
[14] Frenkel, D. and Smit, B. (1996) *Understanding Molecular Simulation* (Academic Press, San Diego).

Downloaded At: 18:29 14 January 2011

[15] Potoff, J.J., Errington, J.R. and Panagiotopoulos, A.Z. (1999) "Molecular simulation of phase equilibria for mixtures of polar and non-polar components", *Mol. Phys.* **97**, 1073.
[16] Bourasseau, E., Ungerer, P. and Boutin, A. (2002) "Prediction of equilibrium properties of cyclic alkanes by Monte Carlo simulation—new anisotropic united atoms potential—new transfer bias method", *J. Phys. Chem. B* **106**, 5483.
[17] Cracknell, R.F., Nicholson, D. and Parsonage, N.G. (1990) "Rotational insertion bias: a novel method for simulating dense phases of structured particles, with particular application to water", *Mol. Phys.* **71**, 931.
[18] Kong, C.L. (1973) "Combining rules for intermolecular potential parameters. II. Rules for the Lennard–Jones (12–6) potential and the Morse potential", *J. Chem. Phys.* **59**, 2464.
[19] Delhommelle, J. and Millié, P. (2001) "Inadequacy of the Lorentz–Berthelot combining rules for accurate predictions of equilibrium properties by molecular simulation", *Mol. Phys.* **99**, 619–625.
[20] Jorgensen, W.L. (1986) "Optimized intermolecular potential functions for liquid alcohols", *J. Phys. Chem.* **90**, 1276–1284.
[21] Lagache, M., Ungerer, P., Boutin, A. and Fuchs, A.H. (2001) "Prediction of themodynamic derivative properties of fluids by Monte Carlo simulation", *Phys. Chem. Chem. Phys.* **3**, 4333–4339.
[22] Reid, R.C., Prausnitz, J.M. and Poling, B.E. (1987) *The Properties of Gases and Liquids* (McGraw Hill, New York).
[23] Escobedo, F.A. and Chen, Z. (2001) "Simulation of isoenthalps and Joule–Thomson inversion curves of pure fluids and mixtures", *Mol. Simul.* **26**, 395–416.
[24] Möller, D., Oprzynski, J., Müller, A. and Fischer, J. (1992) "Prediction of thermodynamic properties of fluid mixtures by molecular dynamics simulations: methane–ethane", *Mol. Phys.* **75**, 363.
[25] Neubauer, B., Tavitian, B., Boutin, A. and Ungerer, P. (1999) "Molecular simulations on volumetric properties of natural gas", *Fluid Phase Equilibria* **161**, 45–62.
[26] Errington, J.R. and Panagiotopoulos, A.Z. (1998) "Phase equilibria of the modified Buckingham exp-6 potential from Hamiltonian scaling grand canonical Monte Carlo", *J. Chem. Phys.* **109**, 1093.
[27] Kristof, T. and Liszi, J. (1997) "Effective Intermolecular potential for fluid hydrogen sulfide", *J. Phys. Chem. B* **101**, 5480–5483.
[28] Goodwin, R.D. (1983) *Hydrogen Sulfide Provisional Thermophysical Properties from 188 to 700 K at Pressure to 75 MPa* (National Bureau of Standards, Boulder, CO).
[29] Jorgensen, W.L., Chandrasekhar, J. and Madura, J.D. (1983) "Comparison of simple potential functions for simulating liquid water", *J. Chem. Phys.* **79**, 926–935.
[30] Pablo, J.J.D. and Prausnitz, J.M. (1989) "Phase equilibria for fluid mixtures from Monte Carlo simulation", *Fluid Phase Equilibria* **53**, 177.
[31] Jedlovszky, P. and Vallauri, R. (2001) "Thermodynamic and structural properties of liquid water around the temperature of maximum density in a wide range of pressures: a computer simulation study with a polarizable potential model", *J. Chem. Phys.* **115**, 3750.
[32] Kiyohara, K., Gubbins, K.E. and Panagiotopoulos, A.Z. (1998) "Phase coexistence properties of polarizable water models", *Mol. Phys.* **94**, 803.
[33] Guillot, B. and Guissani, T. (2001) "How to build a better pair potential for water", *J. Chem. Phys.* **114**, 6720.
[34] Vorholz, J., Harismiadis, V.I., Rumpf, B., Panagiotopoulos, A.Z. and Maurer, G. (2000) "Vapor + liquid equilibrium of water, carbon dioxide, and the binary system, water + carbon dioxide, from molecular simulation", *Fluid Phase Equilibria* **170**, 203.
[35] Lisal, M., Smith, W.R. and Nezbeda, I. (2001) "Accurate vapour–liquid equilibrium calculations for complex systems using the reaction Gibbs ensemble Monte Carlo method", *Fluid Phase Equilibria* **181**, 127.
[36] Lisal, M., Kolafa, J. and Nezbeda, I. (2002) "An examination of the five-site potential (TIP5P) for water", *J. Chem. Phys.* **117**, 8892.
[37] Harris, J.G. and Yung, K.H. (1995) "Carbon dioxide's liquid–vapor coexistence curve and critical properties as predicted by a simple molecular model", *J. Phys. Chem.* **99**, 12021–12024.
[38] Vrabec, J., Stoll, J. and Hasse, H. (2001) "A set of molecular models for symmetric quadrupolar fluids", *J. Phys. Chem. B* **105**, 12126–12133.
[39] Graham, C., Imrie, D.A. and Raab, R.E. (1998) "Measurement of the electric quadrupole moments of CO_2, CO, N_2 and BF_3", *Mol. Phys.* **93**, 49–56.
[40] Delhommelle, J., Boutin, A. and Fuchs, A.H. (1999) "Molecular simulation of vapour–liquid coexistence curves for hydrogen sulfide–alkane and carbon dioxide–alkane mixtures", *Mol. Sun.* **22**, 351.
[41] Bourasseau, E., Haboudou, M., Boutin, A., Fuchs, A.H. and Ungerer, P. (2003) "New optimization method for intermolecular potentials—Optimization of a new anisotropic united atoms potential for olefins—Prediction of equilibrium properties", *J. Chem. Phys.* **118**, 3020.
[42] Lide, D.R. (1992) *Handbook of Chemistry and Physics* (CRC Press, Boca Raton, FL).
[43] Peng, D.Y. and Robinson, D.B. (1976) "A new two-constant equation of state", *Ind. Chem. Eng. Fundam.* **15**, 59–64.
[44] Dhima, A., de Hemptinne, J.C. and Moracchini, G. (1998) "Solubility of light hydrocathons and their mixtures in pure water under high pressure", *Fluid Phase Equilibria* **145**, 129–150.
[45] Soave, G. (1972) "Equilibrium constants from a modified Redlich–Kwong equation of state", *Chem. Eng. Sci.* **27**, 1197–1203.
[46] Huron, M.J. and Vidal, J. (1979) "New mixing rules in simple equations of state for representing vapor–liquid equilibria of strongly non-ideal mixtures", *Fluid Phase Equilibria* **1**, 247–265.
[47] Kellermann, S.J., Stouffer, C.E., Eubank, P.T., Holste, J.C., Hall, K.R., Gammon, B.B. and Marsh, K.N. (1995) *Thermodynamic properties of CO_2 + H_2S mixtures, RR-141* (Gas Processors Association, Tulsa).
[48] Soave, G. (1995) "A noncubic equation of state for the treatment of hydrocarbon fluids at reservoir conditions", *Ind. Eng. Chem. Res.* **34**, 3981.
[49] Gray, C.G. and Gubbins, K.E. (1984) *Theory of Molecular Fluids* (Oxford Science, Oxford).
[50] Nieto-Draghi, C., Avalos, J.B. and Rousseau, B. (2003) "Dynamic and structural behavior of different rigid nonpolarizable models of water", *J. Chem. Phys.* **118**, 7954–7964.
[51] Angus, S., Armstrong, B., Reuck, K.M.D., Altunin, V.V., Gadetskii, O.G., Chapela, G.A. and Rowlinson, J.S. (1973) *International Thermodynamic Tables of the Fluid State—Carbon dioxide* (Pergamon, Oxford).

Downloaded At: 18:29 14 January 2011